

Electronic Supplementary Information

**Carbon Fragments as Highly Active Metal-Free Catalysts for Oxygen Reduction
Reaction: A Mechanistic Study**

Keke Mao^{†, ‡, #}, Wei Zhang^{¶, ‡, #}, Jun Dai[‡] and Xiao Cheng Zeng^{*, ‡}

*[†] School of Energy and Environment Science, Anhui University of Technology, Maanshan, Anhui
243032, P. R. China.*

[‡]Department of Chemistry, University of Nebraska, Lincoln, NE 68588, USA

*[¶]Beijing Advanced Innovation Center for Soft Matter Science and Engineering, Beijing University
of Chemical Technology, Beijing 100029, P. R. China*

**Corresponding author. E-mail: xzeng1@unl.edu*

#These authors contributed equally

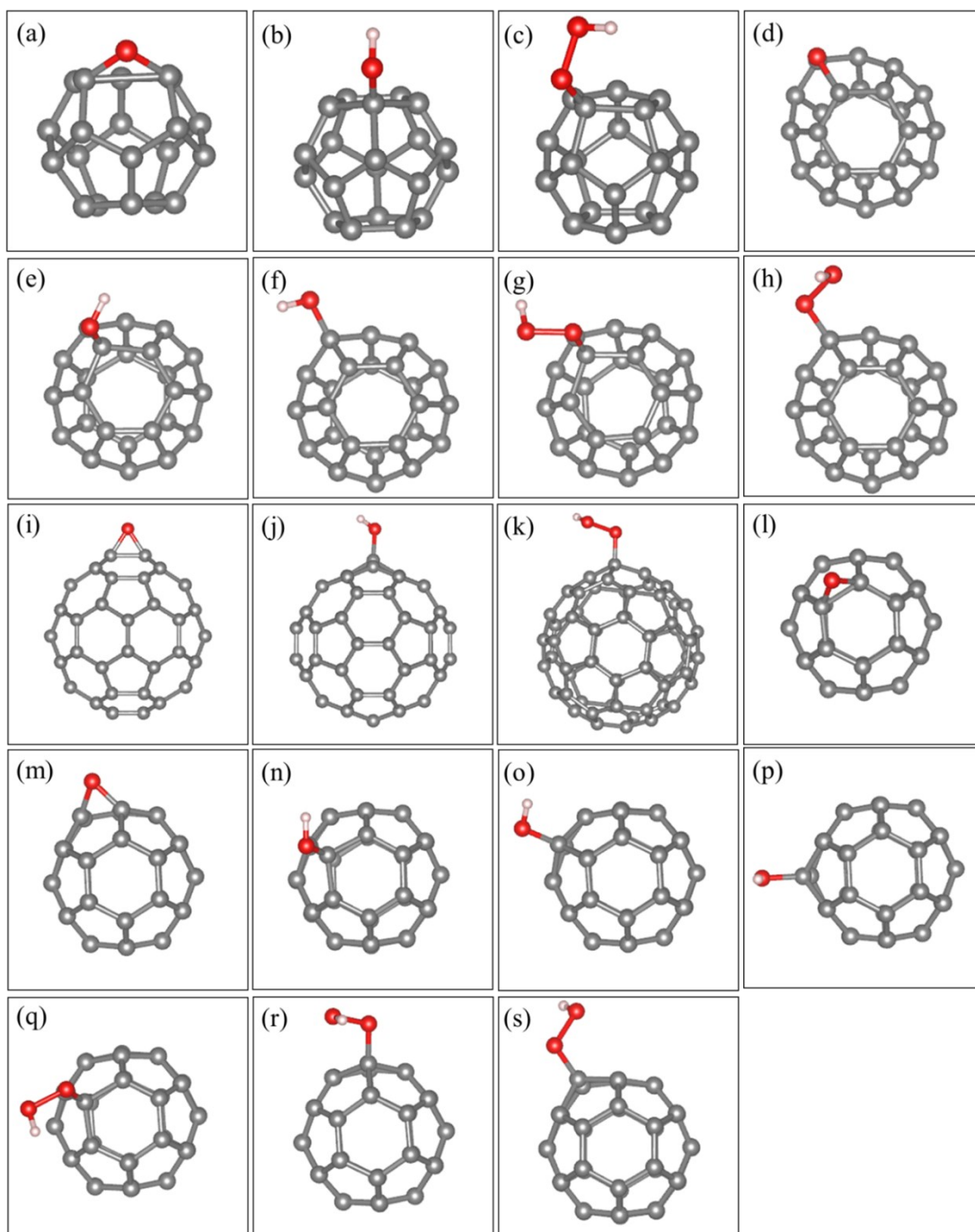


Fig. S1 O^* , OH^* and OOH^* species adsorption configurations on fullerenes. Grey, red, white balls represent carbon, oxygen, hydrogen atoms respectively. **a.** $O@C_{20}$ -3p, **b.** $OH@C_{20}$ -3p, **c.** $OOH@C_{20}$ -3p, **d.** $O@C_{24}$ -3p& C_{24} -2p1h, **e.** $OH@C_{24}$ -2p1h, **f.** $OH@C_{24}$ -3p, **g.** $OOH@C_{24}$ -2p1h, **h.** $OOH@C_{24}$ -3p, **i.** $O@C_{60}$ -1p2h, **j.** $OH@C_{60}$ -1p2h, **k.** $OOH@C_{60}$ -1p2h, **l.** $O@C_{36}$ -2p1h-1, **m.** $O@C_{36}$ -2p1h-2& C_{36} -1p2h, **n.** $OH@C_{36}$ -2p1h-1, **o.** $OH@C_{36}$ -2p1h-2, **p.** $OH@C_{36}$ -1p2h, **q.** $OOH@C_{36}$ -2p1h-1, **r.** $OOH@C_{36}$ -2p1h-2, **s.** $OOH@C_{36}$ -1p2h.

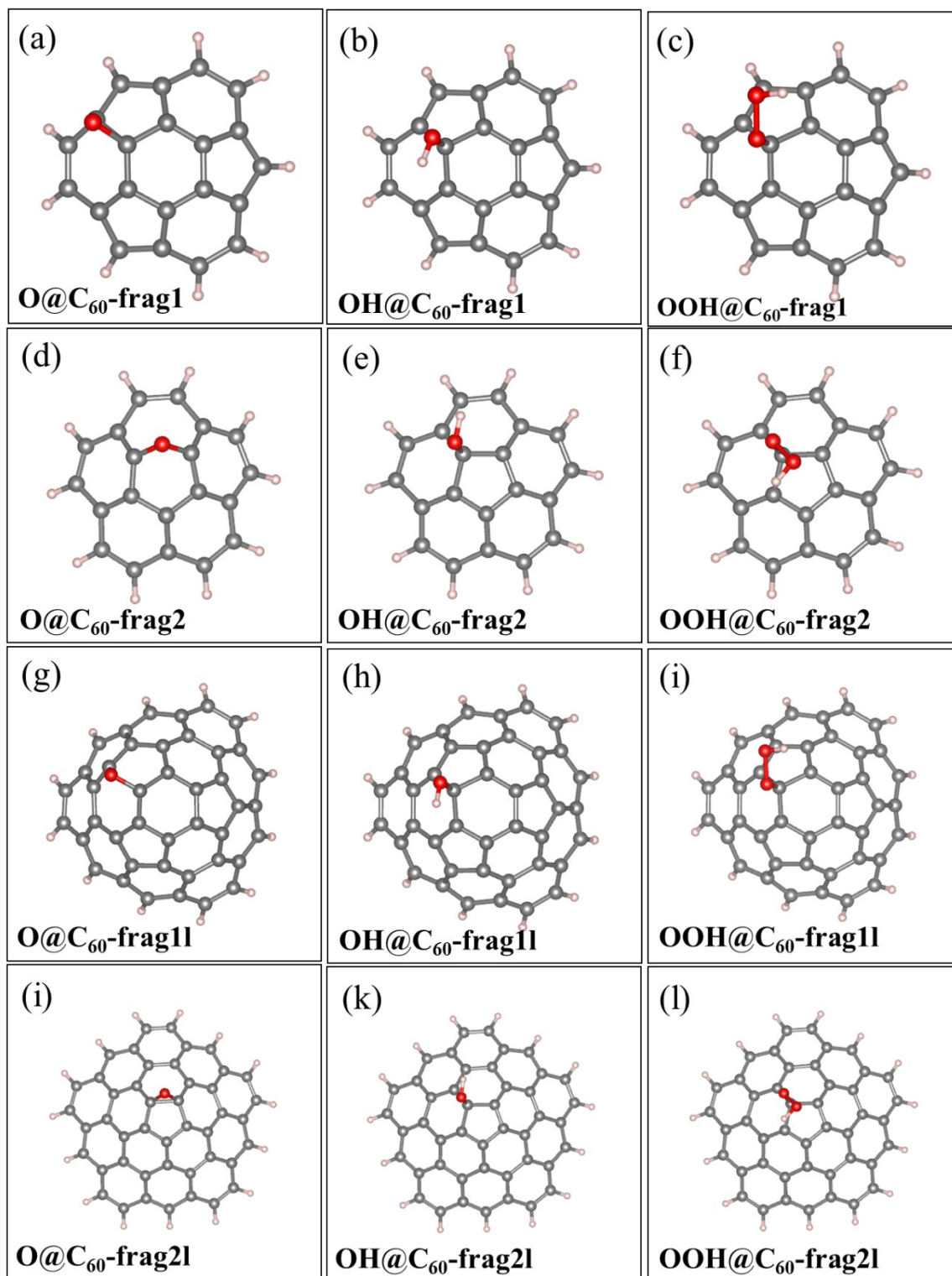


Fig. S2 O^{*}, OH^{*} and OOH^{*} species adsorption configurations on C₆₀-frag1, C₆₀-frag2, C₆₀-frag1l, C₆₀-frag2l four different fragments. Grey, red, white balls represent carbon, oxygen, hydrogen atoms respectively.

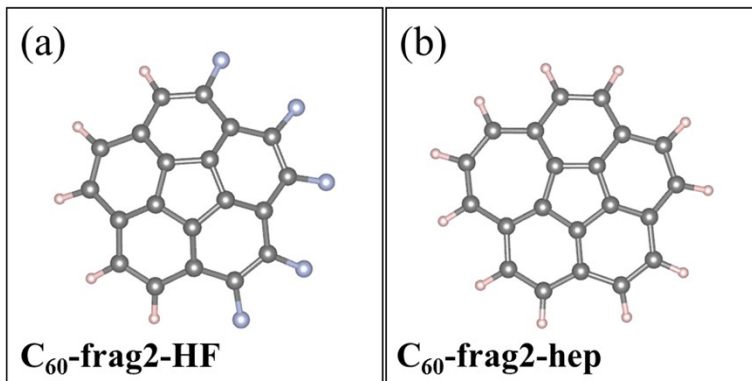


Fig. S3 Two modulated C₆₀-frag2 structures (C₆₀frag2-HF and C₆₀frag2-hep). The grey sphere represents C atom, pink and the blue sphere represent H and fluorine atoms, respectively.

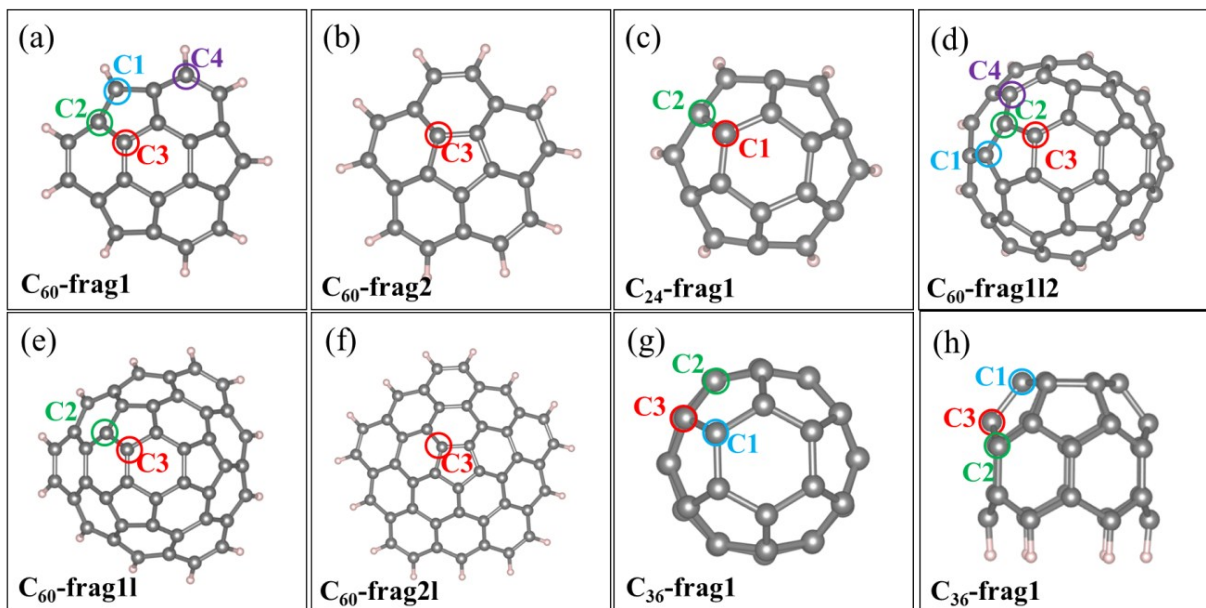


Fig. S4 Various active sites on seven different fullerene-based fragments. C1, C2, C3, and C4 denote four different active sites.

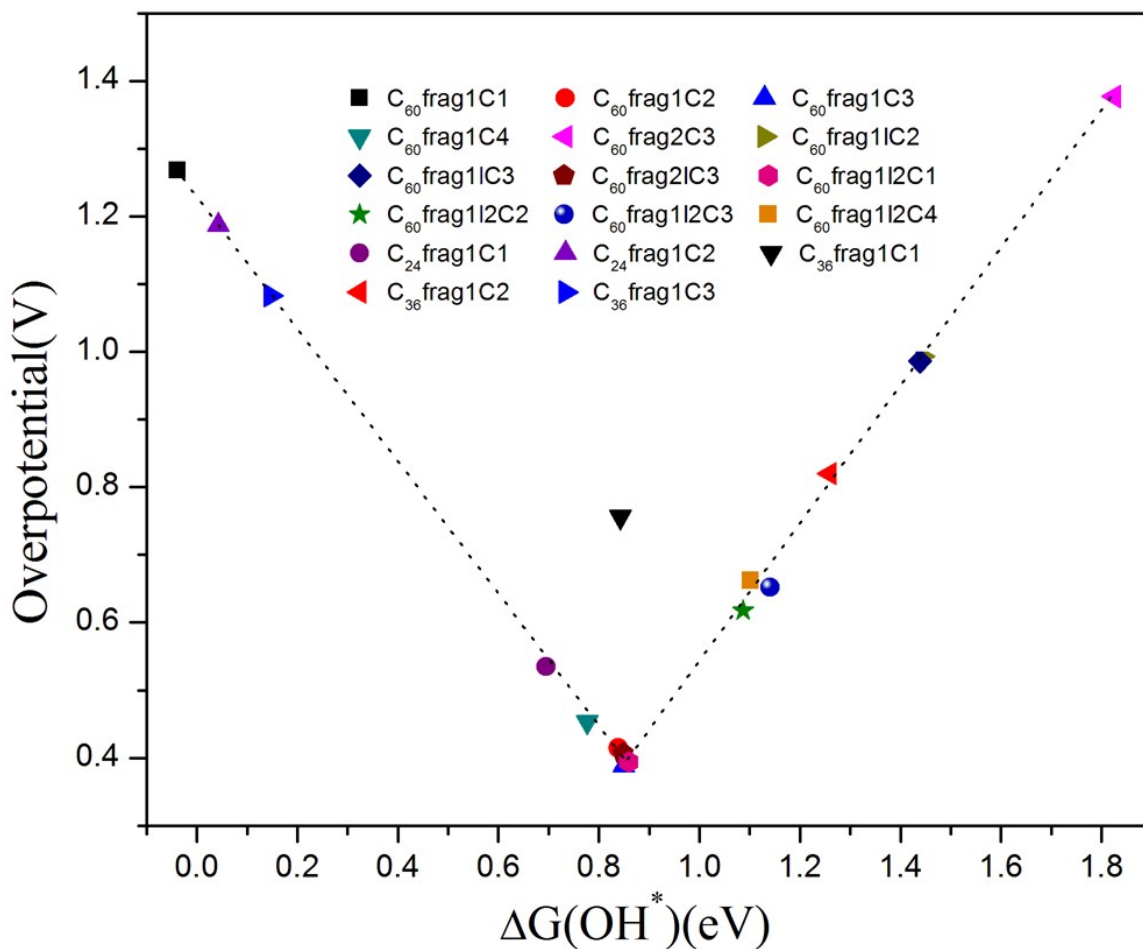


Fig. S5 Trends in oxygen reduction overpotential versus the OH* adsorption free energy.

Table S1 Computed formation energy and formation energy per atom for the four fragments: C₆₀-frag1 and C₆₀-frag2, C₆₀-frag1I and C₆₀-frag2I.

Formation energy	C ₆₀ -frag1	C ₆₀ -frag2	C ₆₀ -frag1I	C ₆₀ -frag2I
E _{form} /eV	-2.235	-5.210	-7.039	-12.382
E _{form} per atom/eV	-0.075	-0.174	-0.130	-0.206

Table S2 $\Delta G(O^*)$, $\Delta G(OH^*)$, and $\Delta G(OOH^*)$ are Gibbs adsorption free energy values (Unit: eV) of key O species (O^* , OH^* and OOH^*) adsorbed on C3 active site of C₆₀-frag1, C₆₀-frag2, C₆₀-frag1l, C₆₀-frag2l fragments. ΔG_1 , ΔG_2 , ΔG_3 , and ΔG_4 are reaction free energy values in each ORR step at U = 0 (Unit: eV). U_{over} is the calculated overpotential of ORR (Unit: V).

	$\Delta G(O^*)$	$\Delta G(OH^*)$	$\Delta G(OOH^*)$	ΔG_1	ΔG_2	ΔG_3	ΔG_4	U_{over}
C ₆₀ -frag1	2.625	0.850	4.079	-0.841	-1.454	-1.775	-0.850	0.389
C ₆₀ -frag2	2.505	1.826	5.067	0.147	-2.562	-0.679	-1.826	1.377
C ₆₀ -frag1l	2.276	1.439	4.676	-0.244	-2.400	-0.837	-1.439	0.986
C ₆₀ -frag2l	2.309	0.848	4.097	-0.823	-1.787	-1.461	-0.848	0.407

Table S3 Computed Bader-charge change before and after the adsorption. For example, $O_{obtained}$ represents the number of electrons O gained after being adsorbed on C₆₀-frag1, C₆₀-frag2, C₆₀-frag1l, or C₆₀-frag2l fragment. C_{loss} corresponds to the lost electrons from the active sites C during the adsorption. O atom is always adsorbed on the bridge site of the two neighboring C atoms, and the Bader-charge change of both C atoms is presented in the table.

Charge e		C ₆₀ -frag1	C ₆₀ -frag2	C ₆₀ -frag1l	C ₆₀ -frag2l
After	O_{gain}	0.891	1.091	1.077	0.860
Adsorb	C_{loss}	0.451, 0.399	0.442, 0.472	0.428, 0.472	0.399, 0.307
After	OH_{gain}	0.480	0.462	0.471	0.471
Adsorb	C_{loss}	0.545	0.474	0.490	0.509
After	OOH_{gain}	0.515	0.477	0.507	0.492
Adsorb	C_{loss}	0.463	0.428	0.444	0.431

Table S4 Free-energy changes associated with C₆₀-frag2 and the two modulated C₆₀-frag2 structures (C₆₀frag2-HF and C₆₀frag2-hep). Computed Gibbs adsorption free energy values (Unit: eV) of key O species O*, OH*, OOH* are denoted as $\Delta G(O^*)$, $\Delta G(OH^*)$, and $\Delta G(OOH^*)$. ΔG_1 , ΔG_2 , ΔG_3 , and ΔG_4 are reaction free energy values in each ORR step at U = 0 (Unit: eV). U_{over} is the calculated overpotential of ORR (Unit: V).

	ΔO^*	ΔOH^*	ΔOOH^*	ΔG_1	ΔG_2	ΔG_3	ΔG_4	U _{over}
C ₆₀ frag2	2.505	1.826	5.067	0.147	-2.562	-0.679	-1.826	1.377
C ₆₀ frag2-HF	2.747	1.786	5.040	0.120	-2.293	-0.961	-1.786	1.350
C ₆₀ frag2-hep	2.692	0.955	4.212	-0.708	-1.520	-1.737	-0.955	0.522

Table S5 Computed free-energy changes on various active sites on seven fragments. Computed Gibbs adsorption free energy values (Unit: eV) of key O species O*, OH*, OOH* are denoted as $\Delta G(O^*)$, $\Delta G(OH^*)$, and $\Delta G(OOH^*)$. ΔG_1 , ΔG_2 , ΔG_3 , and ΔG_4 are reaction free energy values in each ORR step at U = 0 (Unit: eV). U_{over} is the calculated overpotential of ORR (Unit: V).

	$\Delta G(O^*)$	$\Delta G(OH^*)$	$\Delta G(OOH^*)$	ΔG_1	ΔG_2	ΔG_3	ΔG_4	U _{over}
C ₆₀ frag1C1	1.654	-0.038	3.134	-1.786	-1.480	-1.692	0.038	1.268
C ₆₀ frag1C2	1.654	0.839	4.094	-0.826	-2.440	-0.815	-0.839	0.415
C ₆₀ frag1C3	2.625	0.850	4.079	-0.841	-1.454	-1.775	-0.850	0.389
C ₆₀ frag1C4	1.642	0.777	3.986	-0.934	-2.344	-0.865	-0.777	0.453
C ₆₀ frag2C3	2.505	1.826	5.067	0.147	-2.562	-0.679	-1.826	1.377
C ₆₀ frag1lC2	2.102	1.443	4.683	-0.237	-2.582	-0.658	-1.443	0.993
C ₆₀ frag1lC3	2.276	1.439	4.676	-0.244	-2.400	-0.837	-1.439	0.986
C ₆₀ frag2lC3	2.309	0.848	4.097	-0.823	-1.787	-1.461	-0.848	0.407
C ₆₀ frag1l2C1	2.154	0.860	4.084	-0.836	-1.929	-1.295	-0.860	0.394
C ₆₀ frag1l2C2	1.794	1.087	4.308	-0.612	-2.513	-0.707	-1.087	0.618
C ₆₀ frag1l2C3	1.757	1.141	4.342	-0.578	-2.585	-0.616	-1.141	0.652
C ₆₀ frag1l2C4	2.003	1.102	4.352	-0.568	-2.349	-0.901	-1.102	0.662
C ₂₄ frag1C1	1.587	0.695	3.946	-0.974	-2.358	-0.892	-0.695	0.535
C ₂₄ frag1C2	1.066	0.043	3.301	-1.619	-2.234	-1.024	-0.043	1.187
C ₃₆ frag1C1	1.317	0.843	4.092	-0.828	-2.775	-0.474	-0.843	0.756
C ₃₆ frag1C2	1.743	1.260	4.510	-0.410	-2.767	-0.482	-1.260	0.820
C ₃₆ frag1C3	1.317	0.147	3.416	-1.504	-2.099	-1.169	-0.147	1.083